Research Article

Dynamics of a Nonlinear Energy Harvesting System in Time-Delayed Feedback Control under Stochastic Excitations

Shuling Zhang, Ying Zhang [ID], Zhongkui Sun [ID], and Xiaxia Duan

Department of Applied Mathematics, Northwestern Polytechnical University, Xi'an 710072, Shaanxi, China

Correspondence should be addressed to Ying Zhang; yingzhang@nwpu.edu.cn

A time-delayed feedback control is applied to a nonlinear piezoelectric energy harvesting system excited by additive and multiplicative Gaussian white noises to improve its energy harvesting performance. An equivalent decoupling system can be obtained by using a variable transformation. Based on the standard stochastic averaging method, the Fokker–Plank–Kolmogorov equation and the stationary probability density functions of the amplitude, displacement, and velocity of the harvester are obtained, respectively. In addition, the approximate expressions of mean square electric voltage and the mean extracted output power are derived. Finally, the paper explores the influences of parameters on the mean square electric voltage. The results show that noise intensity, time delay, feedback strength, time constant ratio, and coupling coefficients have great influences on the mean square electric voltage. The accuracy of the theoretical method is verified by the Monte Carlo simulation.

1. Introduction

Due to the development of wireless sensors towards low energy consumption and miniaturization, conventional power supply devices are no longer adapted to technological innovation [1, 2]. Nowadays, how to improve the efficiency of an environmental vibration energy harvesting system is becoming a hot research field.

In the recent years, vibration energy harvesters based on the piezoelectric effect have become one of the most effective energy harvesting methods due to their advantages of simple structure, no electromagnetic interference, easy manufacture, and miniaturization [3, 4]. As the first design scheme adopted, a linear vibration energy harvester relies on the resonance phenomenon and has a narrow effective frequency band. Only when the excitation frequency matches its basic natural frequency can it work effectively. A slight perturbation of the basic frequency of a linear harvester to the excitation frequency causes a sharp drop in the energy output [5–7]. Therefore, the linear harvesters based on the resonance principle are not suitable for obtaining energy from broadband and stochastic excitation sources, both of which are typical excitation types in the real world. To

extend the harvester's bandwidth, some recent solutions call for utilizing energy harvesters with stiffness-type nonlinearities. [8–13]. Cottone et al. [14] proposed that the performance of the nonlinear oscillators under stochastic excitation is superior to the linear oscillators through numerical and experimental results. McInnes et al. [15] established the theoretical model of an energy harvesting system based on stochastic resonance and found that its performance was significantly improved. Huang et al. [16] analyzed the dynamical characteristics of the nonlinear vibration energy harvester with an uncertain parameter. Erturk et al. [17, 18] investigated the stochastic response of a bistable energy harvester under harmonic excitation through numerical calculation and experiment. Daqaq [19] explored the stochastic response of the bistable energy harvesting system driven by white noise and exponential correlated Gaussian noise. However, when the bistable energy harvesters are driven by low level excitation, it will not be able to conduct high-energy interwell oscillation. Zhou et al. [20–23] designed a tristable energy harvester, and their results demonstrated that compared to the bistable energy harvester, tri-stable energy harvesters have a smaller high-energy motion threshold and can efficiently collect energy

over a larger low-frequency range. Panyam and Daqaq [24] explored the responses of the tristable energy harvester to harmonic excitation, and the results showed that the tristable energy harvesters have higher output power than the bistable energy harvesters. Huang et al. [25] investigated the resonance mechanism of nonlinear vibrational multistable energy harvesters under narrow-band stochastic parametric excitations.

In fact, vibration energy harvesters are inevitably affected by environmental excitation. Therefore, the researchers investigated the performance of the nonlinear energy harvesting system under stochastic excitation [26–28]. Sun et al. [26] motivated to study stochastic dynamics in a fractional-order system subjected to Gaussian noise. Jin et al. [27] established the semianalytical solution of random response of the nonlinear vibration energy harvester under Gaussian white noise excitation by using generalized harmonic transformation and equivalent nonlinearization. Xiao and Jin [29] explored the energy harvesting of a monostable duffing type harvester with piezoelectric coupling under correlated multiplicative and additive white noise.

Some recent studies have shown that deliberately introducing delay into a continuous-time control dynamical system yields favorable results. In distributed generation systems, the introduction of time delays of a communication network is to ensure the precise voltage restoration and optimal load sharing. [30–32]. Belhaq and Hamdi [33] investigated a delayed van der Pol oscillator with time-varying delay amplitude coupled to an electromagnetic energy harvesting device. Zhang et al. [34] studied the fractional-delay system in the presence of both the colored noise and delayed feedback. Xiao et al. [35, 36] found that the coupling delay provides a strategy to control the oscillating dynamics in fractional-order oscillators. The robust distributed control algorithms consider time-delay communications and noise communication disturbances of a communication network for distributed generation systems.

In general, due to the time required for signal propagation, each electronic equipment inevitably has time delay. However, time delays in both controllers and actuators may deteriorate the control performance or even cause the instability of the piezoelectric energy harvesting system. The appropriate choices of feedback strength and time delays may improve the performance of dynamical systems. However, there are still rarely nonlinear analyses into the energy harvesting enhancement with time-delayed feedback control. Guo et al. [37] proposed a time-delayed feedback control to improve collection performance of the multiple attractors wind-induced vibration energy harvester system. The results show that time-delayed feedback is a powerful tool for achieving a wide range of operating regimes and enhancing amplitude-frequency characteristics and controlling the stochastic or deterministic dynamics of nonlinear systems. However, time-delayed feedback control of the nonlinear piezoelectric energy harvesting system [38, 39] may influence the harvesting performance and the power generation under different excitation conditions, but it has not yet been explored. Therefore, it is necessary to deeply analyze the influences of time-delayed feedback control on the energy harvesting system.

In this paper, the aimed system is a nonlinear piezoelectric energy harvesting system containing time-delayed feedback control in the presence of additive and multiplicative Gaussian white noise. We devote ourselves to studying the stochastic responses induced by time-delayed feedback in the energy harvesting system. It has been found that not only the noise time, constant ratio, and coupling coefficients but also the time delay and the feedback strength can increase the harvested energy from vibrations. The main work and the results are as follows. The piezoelectric energy harvesting system and its equivalent system are given in Section 2. The stationary probability density functions (PDFs) of displacement and velocity are calculated by using the stochastic average method, and the approximate expressions of the mean square electric voltage (MSEV) are derived in Section 3. In addition, the influences of parameters on the MSEV are discussed in detail. Finally, conclusions are drawn in Section 5.

2. Model and the Equivalent System

2.1. Model. A simplified model of a piezoelectric energy harvester is shown in Figure 1 [38, 39]. Through theoretical analysis and experimental measurement, the control electromechanical model of the piezoelectric energy harvesting system is deduced:

$$m\ddot{\overline{X}} + c\dot{\overline{X}} + \delta_1 \overline{X} + \delta_3 \overline{X}^3 + \theta\dot{V} = -m\ddot{\overline{X}}_b, \tag{1}$$

$$C_p \dot{\overline{V}} + \frac{\overline{V}}{R} = \theta\dot{\overline{X}}, \tag{2}$$

where $\overline{X}$ is the displacement of mass m and c, δ_1, and δ_3 are the damping coefficient and the linear and nonlinear stiffness coefficients, respectively. θ is the electromechanical coupling coefficient, C_p is the piezoelectric capacitance, and V is the voltage measured across the equivalent resistive load R.

For simplicity, a set of nondimensionless parameters is introduced as

$$\begin{aligned} X &= \frac{\overline{X}}{l_c}, \\ t &= \omega_1 \tau, \\ \omega_1 &= \sqrt{\frac{\delta_1}{m}}, \\ \lambda &= \frac{\delta_3 l_c^2}{\delta_1}, \\ V &= \frac{C_p}{l_c \theta} \overline{V}, \\ \xi &= \frac{c}{2\sqrt{\delta_1 m}}, \\ \kappa &= \frac{\theta^2}{C_p k_1}, \\ \alpha &= \frac{1}{RC_p \omega_1}. \end{aligned} \tag{3}$$
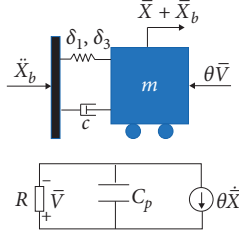
FIGURE 1: A simplified model of a piezoelectric energy harvester.

The nonlinear piezoelectric energy harvesting system is dimensionless as follows:

$$\ddot{X} + 2\xi\dot{X} + X + \lambda X^3 + \kappa V = -\ddot{X}_b, \tag{4}$$

$$\dot{V} + \alpha V = \dot{X}. \tag{5}$$

On the other hand, time-delayed feedback control $F(t) = u(\dot{X}(t-\tau) - \dot{X}(t))$ is proposed [40]. Meanwhile, the energy harvesting system is inevitably affected by the external environment noise, and the additive and multiplicative Gaussian white noise excitation can more accurately replace the harmonic excitation as the stochastic noise source.

Therefore, the corresponding model with time-delayed feedback control under additive and multiplicative Gaussian white noise is

$$\ddot{X} + 2\xi\dot{X} + X + \lambda X^3 + \kappa V = \xi_1(t) + X\xi_2(t) + u(\dot{X}_\tau - \dot{X}), \tag{6}$$

$$\dot{V} + \alpha V = \dot{X}, \tag{7}$$

where 2ξ is the nondimensional linear damping coefficient. κ is the piezoelectric coupling coefficient in the mechanical equation. λ is the nondimensional nonlinear stiffness coefficient. α is time constant ratio. u is the feedback strength, and τ is the time delay. $\xi_1(t)$ and $\xi_2(t)$ denote Gaussian white noise which have the following properties:

$$\langle \xi_i(t) \rangle = 0, R_{ij}(\tau) = \langle \xi_i(t)\xi_j(t+\tau) \rangle$$
$$= \begin{cases} 2D_{ij}\delta(\tau), & i = j, \\ 0, & i \neq j, \end{cases} \quad i, j = 1, 2, \tag{8}$$

where D_{11} and D_{22} are the Gaussian white noise intensities of $\xi_1(t)$ and $\xi_2(t)$, respectively.

2.2. The Equivalent System. Supposing that the noise excitation intensity, damping coefficient, and cubic nonlinear term coefficient are small, the responses of equation (6) can be regarded as stochastic disturbance of periodic solutions about a conservative linear system. Therefore, assume that the solution of system (5) has the following form [41, 42]:

$$X(t) = A(t) \quad \Phi,$$
$$\dot{X}(t) = -A(t)\omega_0 \sin \Phi, \tag{9}$$

where $\Phi(t) = \omega_0 t + \theta(t)$, $A(t)$ is the amplitude, and $\Phi(t)$ is the phase angle.

Substituting equation (9) into equation (6) yields [43]

$$V(t) = C(t)e^{-\alpha t} + \frac{A\omega_0}{\alpha^2 + \omega_0^2}(\omega_0 \cos \Phi - \alpha \sin \Phi). \tag{10}$$

The stationary part of equation (10) is

$$V(t) = \frac{A\omega_0}{\alpha^2 + \omega_0^2}(\omega_0 \cos \Phi - \alpha \sin \Phi)$$
$$= \frac{\omega_0^2}{\alpha^2 + \omega_0^2}X(t) + \frac{\alpha}{\alpha^2 + \omega_0^2}\dot{X}(t). \tag{11}$$

As

$$\omega_0 \cos \Phi - \alpha \sin \Phi = \sqrt{\alpha^2 + \omega_0^2}\cos\left(\Phi + \tan^{-1}\frac{\alpha}{\omega_0}\right), \tag{12}$$

the amplitude of the stationary voltage can be obtained as

$$L = \frac{A\omega_0}{\sqrt{\alpha^2 + \omega_0^2}}. \tag{13}$$

Then,

$$\dot{X}_\tau = \dot{X}(t-\tau) = -A(t-\tau)\omega_0 \sin(\omega_0(t-\tau) + \theta(t-\tau)),$$
$$= -A(t)\omega_0 \sin \Phi \cos(\omega_0\tau) + A(t)\omega_0 \sin(\omega_0\tau)\cos \Phi,$$
$$= \cos(\omega_0\tau)\dot{X} + \omega_0 \sin(\omega_0\tau)X. \tag{14}$$

Substitution of equations (11) and (14) into equation (6) yields a modified decoupling equation:

$$\ddot{X} + S\dot{X} + \omega^2 X + \lambda X^3 = \xi_1(t) + X\xi_2(t), \tag{15}$$

where $\omega^2 = 1 + (\kappa\omega_0^2/\alpha^2 + \omega_0^2) - u\omega_0 \sin(\omega_0\tau)$ and $S = 2\xi + (\kappa\alpha/\alpha^2 + \omega_0^2) - u\cos(\omega_0\tau) + u$.

3. Theoretical Analysis

Using the stochastic average method, suppose the responses of equation (15) can be expressed as follows [44]:

$$X(t) = A(t)\cos \Phi,$$
$$\dot{X}(t) = -A(t)\omega \sin \Phi, \tag{16}$$
$$\Phi(t) = \omega t + \Theta(t).$$

Substituting equation (16) into equation (15) yields

$$\dot{A} = \frac{1}{\omega}\left(-A\omega S \sin \Phi + \lambda A^3 \cos^3 \Phi\right)\sin \Phi$$
$$- \frac{1}{\omega}\xi_1(t)\sin \Phi - \frac{1}{\omega}\xi_2(t)A\cos \Phi \sin \Phi, \tag{17}$$

$$\dot{\Theta} = \frac{\cos \Phi}{A\omega}\left(-A\omega S \sin \Phi + \lambda A^3 \cos^3 \Phi\right)$$
$$- \frac{1}{A\omega}\xi_1(t)\sin \Phi - \frac{1}{A\omega}\xi_2(t)A\cos \Phi \sin \Phi. \tag{18}$$

By adopting the standard stochastic averaging method, the stochastic differential equation (in the Ito sense) for the instantaneous amplitude $A(t)$ is determined by

$$dA = m(A)dt + \sigma(A)dW(t), \qquad (19)$$

where $W(t)$ is an independent normalized Wiener process. (A, Θ) can be approximated as the two-dimensional stochastic diffusion process. The drift coefficient and diffusion coefficient of the Fokker–Plank–Kolmogorov (FPK) equation can be obtained as follows:

$$m(A) = \left\langle \begin{array}{c} -AS\sin^2\Phi + \dfrac{\lambda}{\omega^2}A^3\cos^3\Phi\sin\Phi \\[2mm] +\dfrac{1}{A\omega^2}\left[\begin{array}{c} D_{11}\cos^2\Phi - I_{11}(\omega)\cos\Phi\sin\Phi \\ +D_{22}A^2\cos^4\Phi - A^2\cos^3\Phi\sin\Phi I_{22}(2\omega) \end{array} \right] \end{array} \right\rangle_\Phi, \qquad (20)$$

$$\sigma^2(A) = \left\langle \frac{2D_{11}}{\omega^2}\sin^2\Phi + \frac{2D_{22}A^2\cos^2\Phi}{\omega^2}\sin^2\Phi \right\rangle_\Phi, \qquad (21)$$

where $\langle\rangle_\Phi = \lim\limits_{T\to\infty}(1/T)\int_0^T \langle\rangle dt = (1/2\pi)\int_0^{2\pi} d\Phi$. $S(\omega)$ and $I(\omega)$ have the following form:

$$
\begin{aligned}
S(\omega) &= \frac{1}{\pi}\int_{-\infty}^{0}\cos(\omega t)R(\tau)d\tau, \\
I(\omega) &= \frac{1}{\pi}\int_{-\infty}^{0}\sin(\omega t)R(\tau)d\tau.
\end{aligned} \qquad (22)
$$

Obviously, the amplitude A does not depend on the phase Θ. In conclusion, the FPK equation of amplitude A yields

$$\frac{\partial p}{\partial t} = -\frac{\partial}{\partial A}(m(A)p) + \frac{1}{2}\frac{\partial^2}{\partial A^2}(\sigma^2(A)p). \qquad (23)$$

In the stationary sense, equation (23) can be solved to yield the stationary PDFs for amplitude

$$p(A) = \frac{C}{\sigma^2(A)}\exp\left(\int_0^A \frac{m(u)}{\sigma^2(u)}du\right), \qquad (24)$$

in which C is a normalization factor.

The joint PDF of the amplitude and phase can be retrieved as

$$p(A, \Theta) = p(A)p(\Theta) = \frac{1}{2\pi}p(A). \qquad (25)$$

According to the transformation from (A, Θ) to the $(X, \dot{X})$, we can obtain the expression of the joint PDF of X and $\dot{X}$ as follows:

$$p(X, \dot{X}) = \frac{1}{\omega_1 A}p(A, \Theta) = \frac{1}{2\pi\omega_1 A}p(A). \qquad (26)$$

The corresponding marginal stationary PDFs of displacement X and velocity $\dot{X}$ are shown in equations (27) and (28), respectively.

$$p(X) = \int_{-\infty}^{+\infty}p(X, \dot{X})d\dot{X}, \qquad (27)$$

$$p(\dot{X}) = \int_{-\infty}^{+\infty}p(X, \dot{X})dX. \qquad (28)$$

Thus, the expected value of the MSEV and the mean extracted output power are

$$\langle V^2(t)\rangle = \frac{\omega_0^2}{\alpha^2 + \omega_0^2}\langle A^2\rangle = \frac{\omega_0^2}{\alpha^2 + \omega_0^2}\int_0^{+\infty}A^2 p(A)dA, \qquad (29)$$

$$\langle P\rangle = \alpha k\langle V^2(t)\rangle. \qquad (30)$$

4. Numerical Simulation

In this section, we mainly focus on the influences of the parameters on the stochastic responses of the piezoelectric energy harvesting system. To verify the validity of the analysis results, equations (6) and (7) will be directly simulated by Monte Carlo simulations. Let $\alpha = 0.05$, $\lambda = 0.05$, and the initial conditions are set as the static equilibrium position $X(0) = 0, \dot{X}(0) = 0, V(0) = 0$. The Monte Carlo simulations are selected as the reference to evaluate the accuracy of the analytical results.

4.1. The Influences of Parameters on PDFs. When $\tau = 0.5$, $k = 0.3$, and $u = 0.05$, the stationary PDFs of amplitude, displacement, and velocity under different noise intensities are investigated, as in Figure 2. Specifically, when Gaussian white noise intensity increases continuously, the stationary PDFs peak values decrease and shift to the right, which indicates that the system leads to a large response and gives out a high harvested energy. It can be concluded that the larger excitation intensity plays an important role in the stationary responses of the nonlinear piezoelectric energy harvester. The results are consistent with those of numerical simulation, which can prove the validity of theoretical analysis.

While fixing parameters $D_{11} = 0.02$, $D_{22} = 0.02$, and $\tau = 0.5$, the stationary PDFs of the amplitude, displacement, and the velocity for different feedback strengths are demonstrated in Figure 3. As the feedback strength increases from negative to positive, the shape of the stationary PDFs become steeper gradually, which results in the probability of the system stabilizing at the equilibrium position increasing. It can be clearly explained that under this set of parameters, negative feedback intensity is more conducive to the energy harvester. According to Figures 2 and 3, we can conclude that the results obtained by the theoretical method are consistent well with those from Monte Carlo simulations.

4.2. The Influences of Parameters on the MSEV. In order to completely clarify the influences of the parameters on the performance of the piezoelectric energy harvesters, noise intensity, feedback strength, and time delay are successively introduced to investigate their influences on MSEVs in the following analysis. By taking $u = -0.05$, $k = 0.5$, and $\tau = 0.5$, the effects of additive and multiplicative Gaussian white noise intensity on the MSEV are illustrated in Figures 4(a) and 4(b), respectively. It is found that with the increase of the additive and multiplicative noise intensity, MSEVs increase
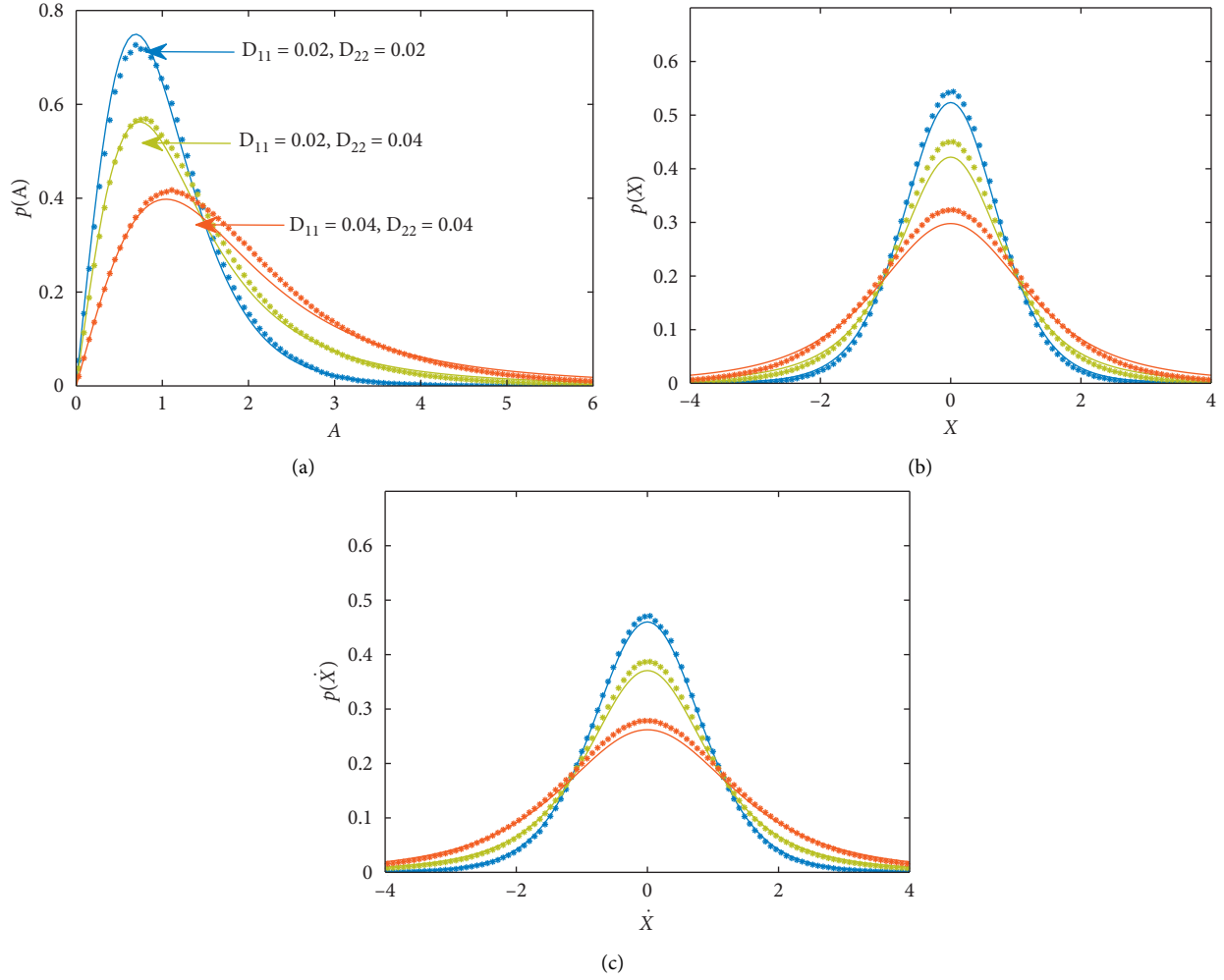
(a)

(b)

(c)

FIGURE 2: The stationary PDFs under different noise intensities: (a) amplitude, (b) displacement, and (c) velocity. Theoretical analysis results (-) and Monte Carlo simulation results (∗).

monotonically. The results show that additive noise plays a leading role in energy harvesting. The energy extracted from multiplicative noise by the piezoelectric energy harvester is relatively small, but it still makes sense when the noise intensity is large. Therefore, appropriately increasing the additive and multiplicative excitation intensity is a feasible method to increase the output voltage.

The variation of the MSEV with the time delay and feedback strength is illustrated in Figure 5. It is seen that for any time delay τ, the MSEV $\langle V^2 \rangle$ increases monotonically with the decrease of the feedback strength u. Nevertheless, the influences of time delay on the MSEV are nonmonotone.

To illustrate the influences of the feedback strength on MSEV, Figure 6(a) shows the changing of the MSEV with the feedback strength $u = 0.01$ and $u = -0.01$. For $D_{11} = 0.02$, $D_{22} = 0.02$, and $k = 0.5$, the variation of the MSEV $\langle V^2 \rangle$ over the time delay τ is investigated. The results show that MSEV of the energy harvesting system without delay feedback system can be stabilized at 0.51. When $u = -0.01$, the time delay τ reaches the critical value of 3.14, and the

MSEV of the system reaches the maximum and then decreases monotonically. However, when the feedback strength $u = 0.01$, the curve of the MSEV changing with time delay τ seems to be completely opposite. For $\tau < 3.14$, the MSEV decreases monotonically as the time delay increases. When $\tau > 3.14$, the MSEV increases with the continuous increase of time delay. Furthermore, negative feedback strength is more favorable to the energy harvesting system than positive feedback strength. Therefore, the harvesting efficiency of the energy harvesting system can be improved by selecting the optimal control parameters u and τ.

By taking $D_{11} = 0.02$, $D_{22} = 0.02$, and $\tau = 1$, the dependence of the MSEV $\langle V^2 \rangle$ on feedback strength u and time constant ratio α is depicted in Figure 7(a). Specifically, the MSEV decreases rapidly as the time constant ratio α increases for a negative feedback strength $u = -0.02$. However, the MSEV decreases slowly with the increase of the time constant ratio for a positive feedback strength $u = 0.02$. As the time constant ratio continues to increase, both the positive and negative feedback strengths keep the MSEV in a
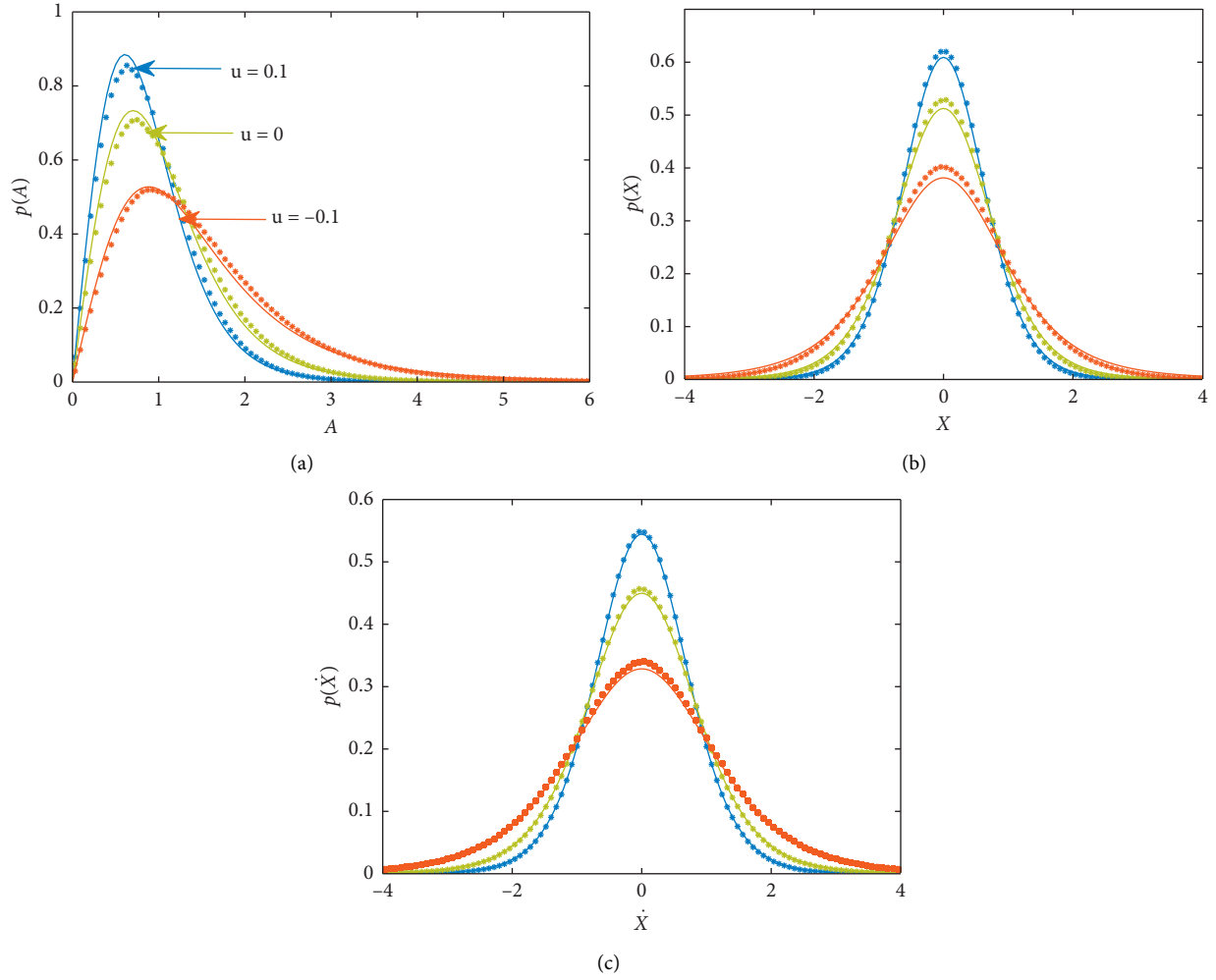
FIGURE 3: The stationary PDFs under feedback strength. (a) Amplitude, (b) displacement, and (c) velocity. Theoretical analysis results (-) and Monte Carlo simulation results (∗).
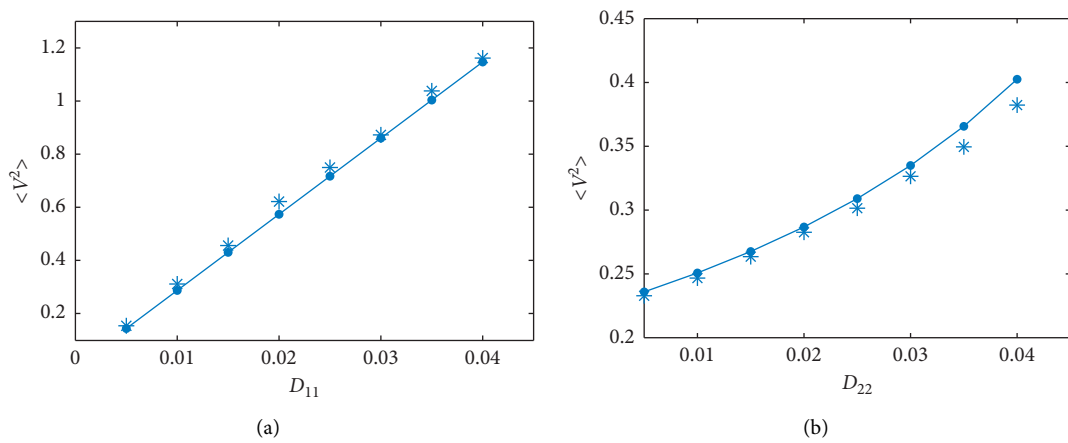

FIGURE 4: The influences of noise intensity on the MSEV. Theoretical analysis results (solid round) and Monte Carlo simulation results (∗).

small range. Through the abovementioned analysis, a smaller time constant ratio and the negative feedback control will make the energy harvesting system induce larger MSEV.

The influences of the MSEV $\langle V^2 \rangle$ on feedback strength u and the piezoelectric coupling coefficient κ are shown in Figure 8. The MSEV almost decreases proportionally with
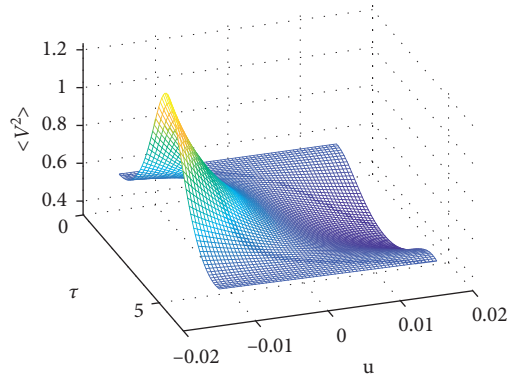
Figure 5: The influences of time delay and feedback strength on the MSEV.
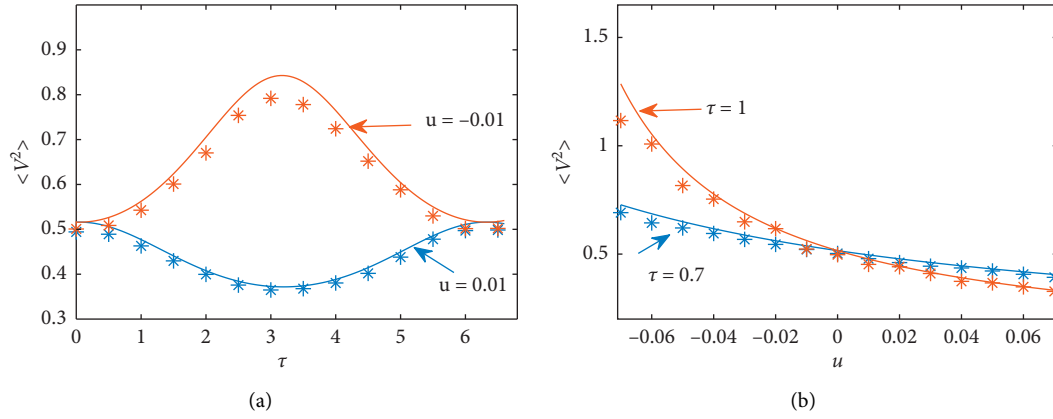

(a)

(b)

Figure 6: The influences of time delay and feedback strength on the MSEV. Theoretical analysis results (solid line) and Monte Carlo simulation results (∗).
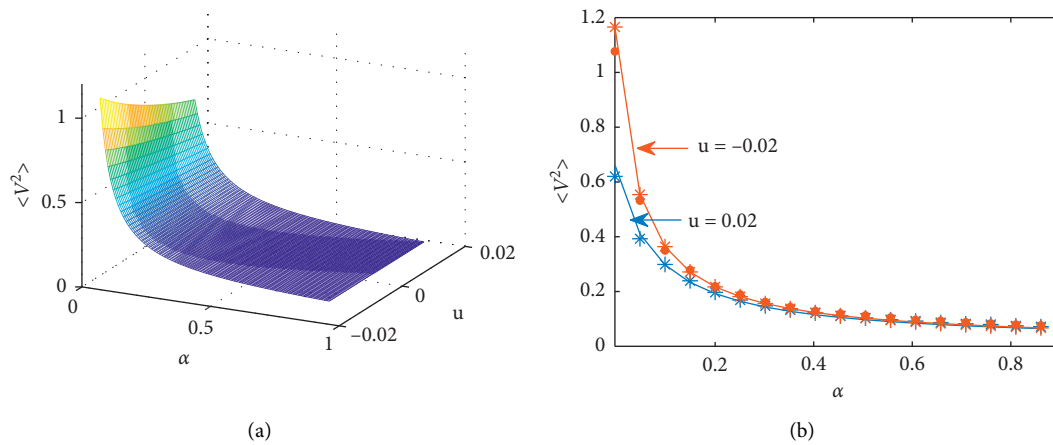

(a)

(b)

Figure 7: The influences of time delay and feedback strength on the MSEV. Theoretical analysis results (solid line) and Monte Carlo simulation results (∗).
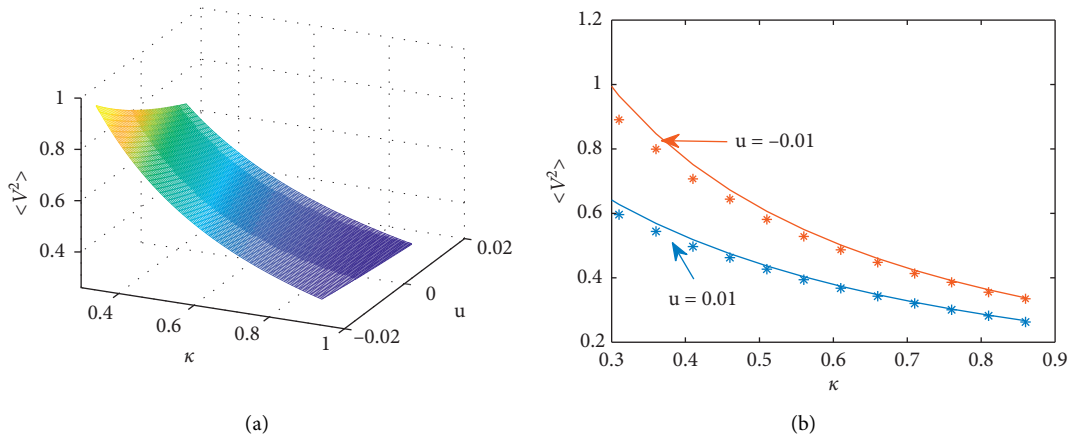
(a)

(b)

FIGURE 8: The influences of piezoelectric coupling coefficient and feedback strength on the MSEV. Theoretical analysis results (solid line) and Monte Carlo simulation results (∗).

the increases of κ at any feedback strength u in Figure 8(b). This means a smaller κ and the negative feedback control will increase the production of output power.

5. Conclusions

In this paper, the time-delayed feedback control is utilized to improve the efficiency of a nonlinear piezoelectric energy harvesting system under the influences of the additive and multiplicative Gaussian white noise excitation. The standard stochastic averaging method has been applied to derive the stationary PDFs of amplitude, displacement, and velocity. Then, the expression of MSEV is deduced via the approximate relationship between voltage and mechanical states. Furthermore, the influences of the parameters on the MSEV are investigated. The results show that the efficiency of the harvester can be improved by selecting the optimal time delay and negative feedback strength when the other parameters unaltered. Moreover, the increases of noise intensity will lead to the increases of MSEV. Besides, we find that time constant ratio and coupling coefficients will reduce the MSEV. The analysis results are almost consistent with the Monte Carlo simulation results of the original system, which verifies the rationality and validity of the theoretical method.

Compared with the nonlinear monostable, the multistable piezoelectric energy harvesting systems have attracted much attention due to the activation of the large-orbit interwell snap-through mechanism. Therefore, we will focus on the bistable energy harvesting system with the time-delayed feedback control next steps.

Data Availability

The data used to support the findings of the study are available from the corresponding author upon request.

Conflicts of Interest

The authors declare that there are no conflicts of interest concerning the publication of this article.

References

[1] C. Liang, J. Ai, and L. Zuo, "Design, fabrication, simulation and testing of an ocean wave energy converter with mechanical motion rectifier," *Ocean Engineering*, vol. 136, pp. 190–200, 2017.

[2] Y. Kuang and M. Zhu, "Characterisation of a knee-joint energy harvester powering a wireless communication sensing node," *Smart Materials and Structures*, vol. 25, no. 5, Article ID 055013, 2016.

[3] N. Elvin and A. Erturk, *Advances in Energy Harvesting Methods*, Springer, Berlin, Germany, 2013.

[4] A. Erturk and D. J. Inman, *Piezoelectric Energy Harvesting*, John Wiley & Sons, Hoboken, NJ, USA, 2011.

[5] S. Roundy and P. K. Wright, "A piezoelectric vibration based generator for wireless electronics," *Smart Materials and Structures*, vol. 13, no. 5, pp. 1131–1142, 2004.

[6] N. E. Dutoit, B. L. Wardle, and S. G. Kim, "Design considerations for memsscale piezoelectric mechanical vibration energy harvesters," *Integrated Ferroelectrics*, vol. 71, no. 1, pp. 121–160, 2005.

[7] A. Erturk and D. J. Inman, "A distributed parameter electromechanical model for cantilevered piezoelectric energy harvesters," *Journal of Vibration and Acoustics*, vol. 130, no. 4, Article ID 041002, 2004.

[8] B. P. Mann and N. D. Sims, "Energy harvesting from the nonlinear oscillations of magnetic levitation," *Journal of Sound and Vibration*, vol. 319, no. 1-2, pp. 515–530, 2009.

[9] B. P. Mann and B. A. Owens, "Investigations of a nonlinear energy harvester with a bistable potential well," *Journal of Sound and Vibration*, vol. 329, no. 9, pp. 1215–1226, 2010.

[10] T. D. Mbong, M. S. Siewe, and C. Tchawoua, "Controllable parametric excitation effect on linear and nonlinear vibrational resonances in the dynamics of a buckled beam," *Communications in Nonlinear Science and Numerical Simulation*, vol. 54, pp. 377–388, 2018.

[11] D. Mallick, A. Amann, and S. Roy, "Surfing the high energy output branch of nonlinear energy harvesters," *Physical Review Letters*, vol. 117, no. 19, Article ID 197701, 2016.

[12] L. Q. Chen, W. A. Jiang, M. Panyam, and M. F. Daqaq, "A broadband internally resonant vibratory energy harvester," *Journal of Vibration and Acoustics*, vol. 138, no. 6, Article ID 061007, 2016.

[13] G. Sebald, H. Kuwano, D. Guyomar, and B. Ducharne, "Experimental duffing oscillator for broadband piezoelectric energy harvesting," *Smart Materials and Structures*, vol. 20, no. 10, Article ID 102001, 2011.

[14] F. Cottone, H. Vocca, and L. Gammaitoni, "Nonlinear energy harvesting," *Physical Review Letters*, vol. 102, no. 8, Article ID 080601, 2009.

[15] C. R. McInnes, D. G. Gorman, and M. P. Cartmell, "Enhanced vibrational energy harvesting using nonlinear stochastic resonance," *Journal of Sound and Vibration*, vol. 318, no. 4-5, pp. 655–662, 2008.

[16] D. M. Huang, S. X. Zhou, Q. Han, and G. Litak, "Response analysis of the nonlinear vibration energy harvester with an uncertain parameter," *Proceedings of the Institution of Mechanical Engineers, Part K: Journal of Multi-Body Dynamics*, vol. 16, no. 2, pp. 393–407, 2019.

[17] A. Erturk, J. Hoffmann, and D. J. Inman, "A piezomagnetoelastic structure for broadband vibration energy harvesting," *Applied Physics Letters*, vol. 94, no. 25, Article ID 254102, 2009.

[18] A. Erturk and D. J. Inman, "Broadband piezoelectric power generation on high-energy orbits of the bistable Duffing oscillator with electromechanical coupling," *Journal of Sound and Vibration*, vol. 330, no. 10, pp. 2339–2353, 2011.

[19] M. F. Daqaq, "Transduction of a bistable inductive generator driven by white and exponentially correlated Gaussian noise," *Journal of Sound and Vibration*, vol. 330, no. 11, pp. 2554–2564, 2011.

[20] S. Zhou, J. Cao, D. J. Inman, J. Lin, S. Liu, and Z. Wang, "Broadband tristable energy harvester: modeling and experiment verification," *Applied Energy*, vol. 133, pp. 33–39, 2014.

[21] S. Zhou and L. Zuo, "Nonlinear dynamic analysis of asymmetric tristable energy harvesters for enhanced energy harvesting," *Communications in Nonlinear Science and Numerical Simulation*, vol. 61, pp. 271–284, 2018.

[22] J. Cao, S. Zhou, W. Wang, and J. Lin, "Influence of potential well depth on nonlinear tristable energy harvesting," *Applied Physics Letters*, vol. 106, no. 17, Article ID 173903, 2015.

[23] S. Zhou, J. Cao, D. J. Inman, J. Lin, and D. Li, "Harmonic balance analysis of nonlinear tristable energy harvesters for performance enhancement," *Journal of Sound and Vibration*, vol. 373, pp. 223–235, 2016.

[24] M. Panyam and M. F. Daqaq, "Characterizing the effective bandwidth of tri-stable energy harvesters," *Journal of Sound and Vibration*, vol. 386, pp. 336–358, 2017.

[25] D. M. Huang, S. X. Zhou, and Z. C. Yang, "Resonance mechanism of nonlinear vibrational multistable energy harvesters under narrow-band stochastic parametric excitations," *Complexity*, vol. 2019, Article ID 1050143, 20 pages, 2019.

[26] Z. Sun, P. Dang, and W. Xu, "Detecting and measuring stochastic resonance in fractional-order systems via statistical complexity," *Chaos, Solitons & Fractals*, vol. 125, pp. 34–40, 2019.

[27] X. Jin, Y. Wang, M. Xu, and Z. Huang, "Semi-analytical solution of random response for nonlinear vibration energy harvesters," *Journal of Sound and Vibration*, vol. 340, pp. 267–282, 2015.

[28] M. Su, W. Xu, and Y. Zhang, "Theoretical analysis of piezoelectric energy harvesting system with impact under random excitation," *International Journal of Non-linear Mechanics*, vol. 119, Article ID 103322, 2020.

[29] S. Xiao and Y. Jin, "Response analysis of the piezoelectric energy harvester under correlated white noise," *Nonlinear Dynamics*, vol. 90, no. 3, pp. 2069–2082, 2017.

[30] J. G. Lai, X. Q. Lu, X. H. Yu, M. Antonello, and H. Hong, "Distributed voltage regulation for cyber-physical microgrids with coupling delays and slow switching topologies," *IEEE Transactions on Systems, Man, and Cybernetics: Systems*, vol. 50, no. 1, pp. 100–110, 2019.

[31] J. G. Lai, X. Q. Lu, M. Antonello, and G. P. Liu, "Stochastic distributed pinning control for Co-Multi-Inverter networks with A virtual leader," *IEEE Transactions on Circuits and Systems II: Express Briefs*, 2019.

[32] J. G. Lai, X. Q. Lu, X. H. Yu, and M. Antonello, "Stochastic distributed secondary control for ac microgrids via event-triggered communication," *IEEE Transactions on Smart Grid*, vol. 11, no. 4, pp. 2746–2759, 2020.

[33] M. Belhaq and M. Hamdi, "Energy harvesting from quasi-periodic vibrations," *Nonlinear Dynamics*, vol. 86, no. 4, pp. 2193–2205, 2016.

[34] J. Zhang, Z. Sun, X. Yang, and W. Xu, "Controlling bifurcations in fractional-delay systems with colored noise," *International Journal of Bifurcation and Chaos*, vol. 28, no. 11, Article ID 1850137, 2018.

[35] R. Xiao, Z. Sun, X. Yang, and W. Xu, "Amplitude death islands in globally delay-coupled fractional-order oscillators," *Nonlinear Dynamics*, vol. 95, no. 3, pp. 2093–2102, 2019.

[36] R. Xiao, Z. Sun, X. Yang, and W. Xu, "Emergence of death islands in fractional-order oscillators via delayed coupling," *Communications in Nonlinear Science and Numerical Simulation*, vol. 69, pp. 168–175, 2019.

[37] Q. Guo, Z. K. Sun, Y. Zhang, and W. Xu, "Time-delayed feedback control in the multiple attractors wind-induced vibration energy harvesting system," *Complexity*, vol. 2019, Article ID 7973823, 11 pages, 2019.

[38] M. Xu, X. Jin, Y. Wang, and Z. Huang, "Stochastic averaging for nonlinear vibration energy harvesting system," *Nonlinear Dynamics*, vol. 78, no. 2, pp. 1451–1459, 2014.

[39] M. F. Daqaq, "On intentional introduction of stiffness nonlinearities for energy harvesting under white Gaussian excitations," *Nonlinear Dynamics*, vol. 69, no. 3, pp. 1063–1079, 2012.

[40] K. Pyragas, "Continuous control of chaos by self-controlling feedback," *Physics Letters A*, vol. 170, no. 6, pp. 421–428, 1992.

[41] W. Q. Zhu, Z. L. Huang, and Y. Suzuki, "Response and stability of strongly non-linear oscillators under wide-band random excitation," *International Journal of Non-linear Mechanics*, vol. 36, no. 8, pp. 1235–1250, 2001.

[42] J. B. Roberts and P. D. Spanos, "Stochastic averaging: an approximate method of solving random vibration problems," *International Journal of Non-linear Mechanics*, vol. 21, no. 2, pp. 111–134, 1986.

[43] W.-A. Jiang and L.-Q. Chen, "Stochastic averaging of energy harvesting systems," *International Journal of Non-linear Mechanics*, vol. 85, pp. 174–187, 2016.

[44] W. Q. Zhu, Z. L. Huang, and Y. G. Yang, "Stochastic averaging of quasi-integrable Hamiltonian systems," *Journal of Applied Mechanics*, vol. 64, no. 4, pp. 975–984, 1997.